Astron. Astrophys. 338, 1084–1088 (1998)

ASTRONOMY AND ASTROPHYSICS

Chromospheric evaporation shock and reduced optical thickness drifting in the 1-4.5 GHz range

Marian Karlický

Astronomical Institute, Academy of Sciences of the Czech Republic, CZ-251 65 Ondřejov, Czech Republic

Received 11 March 1998 / Accepted 20 July 1998

Abstract. Using a 1-D numerical hydrodynamic model, the evaporation shock evolution is computed in the solar atmosphere having the density profile derived from radioastronomical observations. Then the optical thickness of the 1-4.5 GHz plasma emission on harmonic frequency is computed. It is found that the optical thickness of the radio emission is reduced at the evaporation shock. With a motion of this shock the optical thickness reduction drifts towards lower frequencies with the frequency drift which depends on the evaporation shock speed. The theoretical radio spectrum caused by this optical thickness reduction is presented and discussed in comparison with the July 9, 1996 radio spectrum.

Key words: hydrodynamics – shock waves – Sun: chromosphere – Sun: radio radiation

1. Introduction

It is commonly believed that during the flare impulsive phase, dense layers of the chromosphere are heated by particle beams (Canfield et al. 1980; Somov 1992). Simultaneously, these beams generate hard X-ray bursts. Later on with the time delay of several tens of seconds caused by a slower propagation speed also the thermal conduction can heat these layers. Both types of the heating increase the pressure at these layers, cause evaporation processes and generate evaporation shocks (MacNeice et al. 1984; Mariska et al. 1989; Peres & Reale 1993; Hori et al. 1997). The line broadening and blueshift of soft X-ray lines in Ca XIX and Fe XXV are considered as an evidence of this evaporation process (Antonucci et al. 1982, 1984). The estimated evaporation shock speed is several hundreds km per second. Now, there is a question if the evaporation shock can be detected also by some other means, e.g. on the radio spectrum. In the paper by Aschwanden & Benz (1995) it was suggested that high-frequency slowly drifting cutoffs of decimetric bursts are caused by the evaporation shock. In our paper we start from the same idea, but we include the hydrodynamic simulations, which reveal new aspects of this problem. Moreover, we are interested with a slow negative frequency drift of some 1-4.5 GHz radio bursts observed at the very beginning of flare impulsive phase; an example of the July 9, 1996 event follows. It is shown that this drift can be explained by a presence of the evaporation shock.

Send offprint requests to: M. Karlický

2. Evaporation shock model

Computations of the evaporation shock evolution need initial density and temperature atmospheric profiles. Because we study effects of the evaporation shock on radio spectrum, we prefer to use the density model derived from radioastronomical observations. This model differs from standard VAL or FAL models used in the evaporation shock studies. Namely, the density gradients in the VAL or FAL models do not agree with frequency drifts of type III bursts in the 1-4.5 GHz range. For this reason electron densities in our model were taken the same as in the model by Aschwanden & Benz (1995):

$$n_e(h) = n_1 \left(\frac{h}{h_1}\right)^{-p} \qquad h < h_1, \tag{1}$$

$$n_e(h) = n_Q \exp\left(-\frac{h}{\lambda}\right) \qquad h > h_1, \tag{2}$$

where h is the height in the solar atmosphere, h_1 is the height where the power-law model is changed into the exponentional one, n_1 and n_Q are density constants, p is the power-law index, and λ is the density height scale. From the continuity conditions at height h_1 follow:

$$h_1 = p\lambda, \;\; n_1 = n_Q \exp(-p). \tag{3}$$

As shown by Aschwanden & Benz (1995) the constants p and n_Q can be expressed as:

$$p = \frac{2}{\alpha - 1}, \;\; n_Q = \left(\frac{ev_b}{2A\lambda}\right)^p (s\,8980)^{-2}, \tag{4}$$

where s is the harmonic radiation number, v_b is the beam velocity of type III bursts expressed in units of the speed of light, A and α are constants in the empirical type III drift rate by Alvarez & Haddock (1973): $\partial\nu/\partial t = -A\nu^\alpha$, with α=1.84, and A= 0.01. But in our case we consider the second harmonic radiation s = 2, v_b = 0.25, λ= 6.9 $\times$ 10^9 cm, h_1 = 1.6 $\times$ 10^{10} cm,

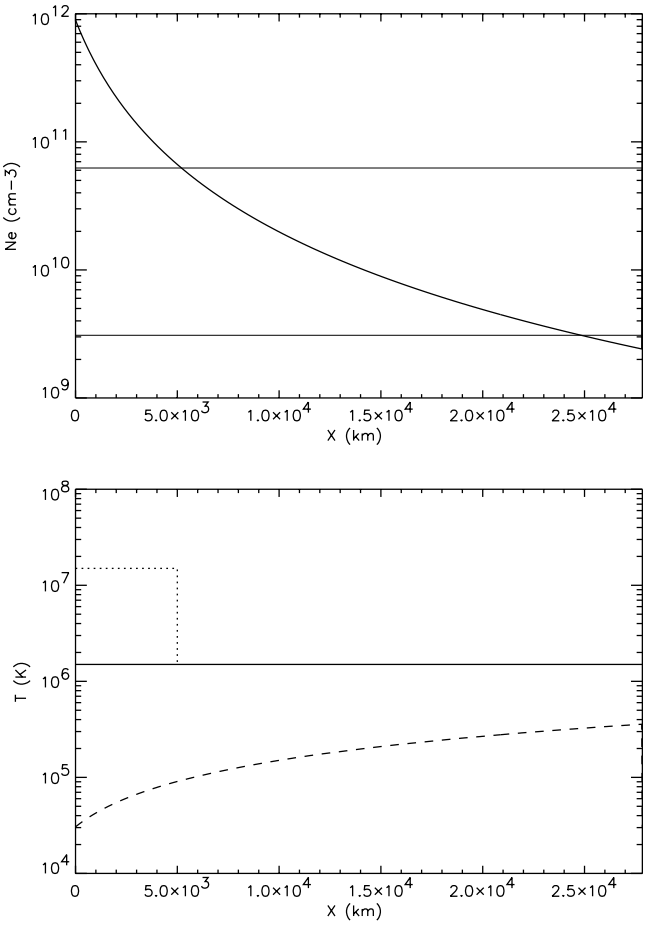

Fig. 1. The initial density and temperature profiles of the flare atmosphere (full lines). The dashed line expresses the equilibrium temperature profile. The evaporation shock is initiated by a temperature jump (dotted line).

and n_Q = 4.6 × 10^8 cm^{-3}, which gives the same density model as that used by Aschwanden & Benz with v_b = 0.14 and s = 1. The initial density profile is shown in Fig. 1.

For numerical computations it is useful if the initial atmosphere is in a gravitational equilibrium, otherwise the atmosphere is evolving. Then the question arises if for the chosen density profile there is a reasonable temperature profile, which gives the atmosphere in equilibrium. Starting from the force equation:

$$-\frac{dP}{dh} - n_e m_p g = 0, \tag{5}$$

where P is the pressure, m_p is the proton mass, g is the gravitational constant, the equilibrium temperature profile can be derived. Expressing the pressure as $P = 2n_e k_B T$, where k_B is the Boltzman constant and using the power-law model for the electron density (relation 1) the differential equation for the temperature T can be written in the form:

$$h\frac{dT}{dh} - pT + Ch = 0, \tag{6}$$

where $C = \frac{m_p g}{2k_B}$. The solution of this equation is

$$T = \frac{1}{(p\lambda)^p}(T_1 - C\frac{p\lambda}{p-1})h^p + \frac{C}{p-1}h, \tag{7}$$

where T_1 is the temperature at height h_1. The equilibrium temperature profile is shown in Fig. 1 by dashed line. But these temperatures are too low compared with typical temperatures in the corona. It means that a reasonable equilibrium temperature profile does not exist and we have to make computations in the non-equilibrium atmosphere. For processes much shorter that the characteristic time of the non-equilibrium state evolution computations are possible. To make a comparison with the studies of Aschwanden & Benz (1995) we assume the initial temperature to be 1.5 MK (see full line in Fig. 1). The numerical simulations of the problem under study is made by the 1-D numerical code (Karlický 1990) which solves a set of the 1-D hydrodynamic equations in the form:

$$\frac{\partial \rho}{\partial t} + \frac{\partial}{\partial h}(\rho v) = 0, \tag{8}$$

$$\frac{\partial}{\partial t}(\rho v) + \frac{\partial}{\partial h}(\rho v^2) = -\frac{\partial P}{\partial h} + \rho g, \tag{9}$$

$$\frac{\partial U}{\partial t} + \frac{\partial}{\partial h}(Uv) = -\frac{\partial}{\partial h}(Pv) + \rho v g, \tag{10}$$

where

$$U = \frac{P}{\gamma - 1} + \frac{1}{2}\rho v^2. \tag{11}$$

In these equations, ρ is the mass density, v is the plasma velocity, and γ is the ratio of specific heats taken to be $\frac{5}{3}$. The radiation losses and thermal conduction are not considered in this case. The bottom boundary condition is fixed, the upper one is free.

The evaporation shock is initiated by the temperature enhancement in space below the 4.5 GHz density limit. We considered several temperature jumps in shocks. Here, we present the case with 15 MK (see the dotted line in Fig. 1), e.g. the case which was considered by Aschwanden & Benz (1995) and that with the typical temperature quoted for the evaporating upflowing plasma from Ca XIX and Fe XXV soft X-ray line measurements (Doschek et al. 1983; Antonucci et al. 1993).

Results of computations, i.e., density, temperature and plasma velocity profiles at 14.07 s after the shock initiation are shown in Figs. 2. The shock velocity is increasing from zero at the initial state up to 1300 km s^{-1} crossing the position of the 1 GHz radiation level.

The shock propagation time between 4.5 and 1 GHz radiation level is 18.73 s. The average shock velocity is 1070 km s^{-1}.

3. Optical thickness of the 1-4.5 GHz plasma emission during the evaporation shock propagation

Now, at specific times of the evaporation shock evolution the optical thickness of the 1-4.5 GHz plasma emission at harmonic frequency is calculated.

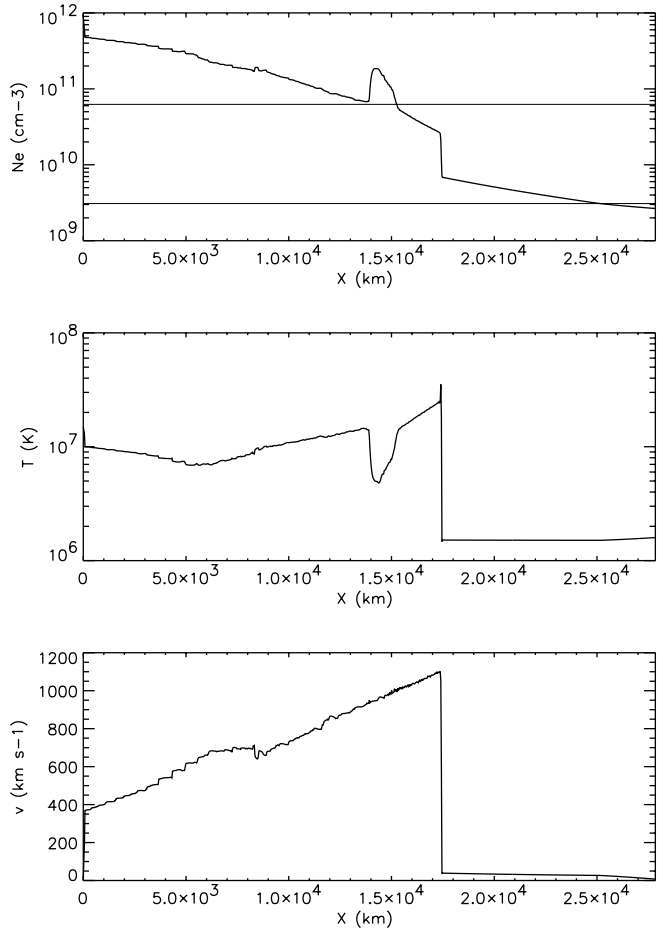

Fig. 2. The density, temperature and plasma velocity profiles of the flare atmosphere at 14.07 s during the evaporation shock propagation.

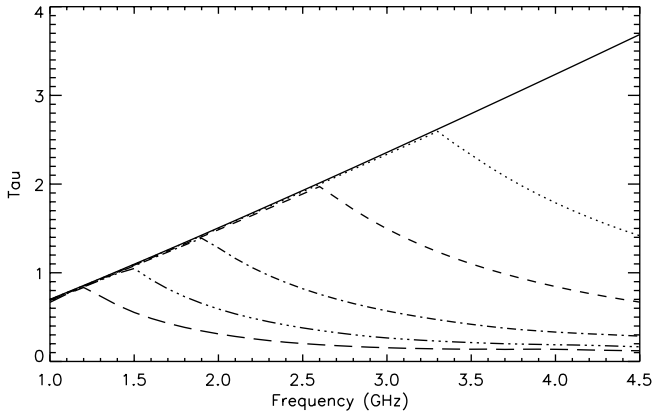

Fig. 3. The optical thickness of the 1-4.5 GHz plasma emission on harmonic frequency during the evaporation shock propagation at 0 s (full line), at 4.91 s (dotted line), at 8.44 s (dashed line), at 11.41 s (dot and dashed line), at 14.07 s (dot-dot-dot and dashed line), and at 16.49 s (long dashed line).

The absorption of emission in the plasma is expressed through the optical thickness τ. The intensity of radiation I is thus attenuated as I=I_0 exp$^{-\tau}$. Generally, the optical thickness is an integral of the absorption along the emission-ray path:

$$\tau = \int_0^X \mu dx, \tag{12}$$

where μ is the absorption coefficient, the radio source is at zero position, and the observer is at X, respectively. This integral can be expressed as (Zheleznyakov 1977)

$$\tau = \int_0^X \frac{\nu_p^2}{\nu^2}\frac{\nu_c}{c} dx, \tag{13}$$

$$\nu_c = \nu_{ei}, \tag{14}$$

$$\nu_{ei} = \frac{5.5 n_e}{T^{3/2}} A, \tag{15}$$

$$A = \ln\left(220\frac{T}{n_e^{1/3}}\right) \qquad T < 4\,10^5 K, \tag{16}$$

$$A = \ln\left(10^4\frac{T^{2/3}}{n_e^{1/3}}\right) \qquad T > 4\,10^5 K, \tag{17}$$

where ν is the radio emission frequency, ν_p is the plasma frequency of the plasma surrounding the radio source, ν_c and ν_{ei} are the collisional and electron-ion collisional frequencies, T is the temperature, n_e is the electron density, and c is the speed of light.

The optical thickness is calculated for the radio emission propagating from the radio source at the corresponding density level upwards into the corona. For this purpose the atmosphere is considered up to the height of 400000 km.

The computed optical thicknesses at 0.0, 4.91, 8.44, 11.41, 14.07, and 16.49 s during the evaporation shock evolution are shown in Fig. 3. Using these optical thicknesses the theoretical radio spectrum is made (Fig. 4). Here, a constant intensity of the radio source I_0 in the 1-4.5 GHz frequency range and time is assumed. The resulting intensity I expressed in the black and white scale in the figure is computed as I = I_0 exp$^{-\tau}$, where τ is the optical thickness.

4. Discussion and conclusions

In the paper we used a very similar model to that of Aschwanden & Benz (1995). But we included hydrodynamic simulations into the model. This model is based on radioastronomical observations. We used this model because effects on the radio spectrum are studied. But, it differs from standard models considered in the evaporation process studies. We found that for this model it does not exist a reasonable equilibrium temperature profile. Our model as well as the model of Aschwanden and Benz are not in the gravitational equilibrium. But for processes under study which are much shorter that the characteristic time of the non-equilibrium state evolution they can be used for computations. Let us assume that just before the flare such a state of the atmosphere is possible (pre-heating phase).

Although in our model we initiated an evaporation shock which is weaker than in the paper by Aschwanden & Benz

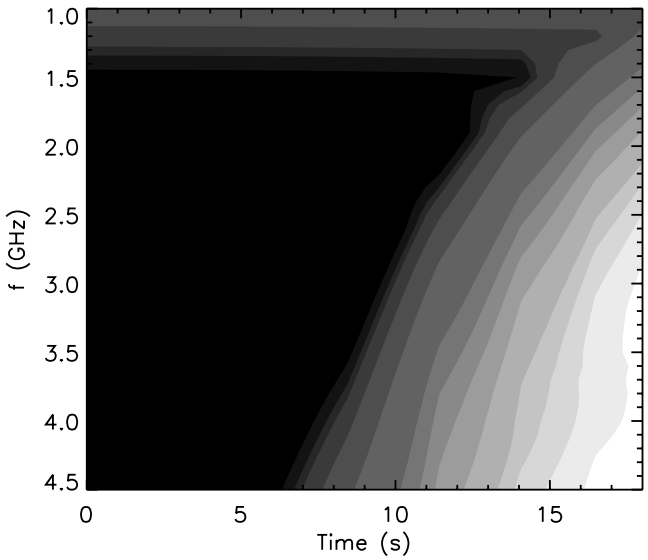

Fig. 4. The 1-4.5 GHz theoretical radio spectrum computed as $I = I_0 \exp^{-\tau}$, where I is the resulting intensity expressed in the black and white scale, I_0 is a constant and τ is the optical thickness.

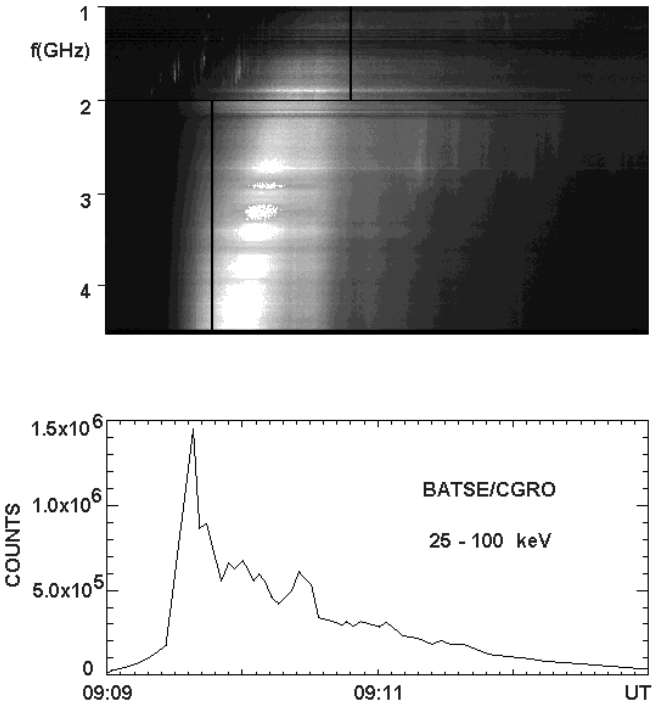

Fig. 5. Upper part: The radio spectrum of high-frequency slowly drifting burst observed during the July 9, 1996 flare by the Ondřejov radiospectrograph. **Bottom part:** The hard X-ray emission observed by BATSE/CGRO experiment.

(1995) (they considered not only the initial temperature shock jump, but also the density shock jump), an inclusion of the hydrodynamic simulation reveals that the shock speed is much higher than that presented in this paper. This fact can be confirmed using the Rankine-Hugoniot relations. The computed shock speed is also higher than that observed (several hundreds km per second) or computed in other similar simulations. Let us compare our results with those computed in the paper by Mariska et al. (1989). In the mentioned paper a maximum plasma velocity in the shock is smaller (650 km s^{-1} at the distance of 8000 km from the initiation space - see the case at 30 s) than in our case (950 km s^{-1} at the moment when the shock is in the same distance). But there is essential difference in the initiation of both shocks. While in our case we consider the sudden temperature enhancement of 15 MK, in the paper of Mariska et al. (1989) the temperature is increasing to the similar values during 30 seconds. In our simplified model this second type of shock initiation corresponds to the simulations with smaller temperature enhancements. We can reconcile our results with observations and other simulations when we use the temperature enhancement of about 3-5 MK (see also following discussions). In such a case the temperature enhancement used in the shock initiation has a meaning of the "effective" one.

It is shown that the evaporation shock causes the frequency drift of the optical thickness reduction in the 1-4.5 GHz radio range. This drift depends on the evaporation shock speed. Thus, there is a drifting window of "visibility" in which the electromagnetic radiation of plasma emission origin can appear. While in the paper of Aschwanden & Benz (1995) the radio emission on the fundamental frequency was considered, we studied this effect for the radio emission on the harmonic frequency, which has higher probability to escape from dense layers of the solar atmosphere.

The presented scenario of the visibility "window" for radio emission drifting towards lover frequencies is valid only at the very beginning of flare, in the phase of the particle beam heating of dense atmospheric layers. Later in the phase of the chromospheric heating by a thermal conduction this scenario must be changed. Namely, the temperature enhancement is propagating downwards from the flare loop top to the chromosphere. In this case the optical thickness reduction drifts towards higher frequencies. Therefore, the effect under study can be seen only at the very beginning of flare. It is known that some flares start with the slowly drifting 1-4.5 GHz burst. The example observed during the July 9, 1996 flare by the Ondřejov radiospectrograph is shown in Fig. 5. The radio burst starts with type III radio bursts at 9:09:20-9:10:10 UT in the 1-2 GHz range indicating particle beams. The presence of nonthermal particles is confirmed also by the hard X-ray emission. Just at this phase we expect the formation of the optical thickness reduction drifting towards lower frequencies (see also the theoretical spectrum, Fig. 4; but in the real spectrum an intensity of the radio source can be strongly variable). Really, in Fig. 5 we can see such a drift in the whole 1-4.5 GHz range at 9:09:30-9:10:30 UT. But this drift is smaller than that in our numerical simulations. The best fit can be obtained for the mean evaporation shock speed of 500 km s^{-1}, i.e. for the temperature enhancement of 3 MK for the shock initiation. Although the interpretation of the slow drift of the 1-4.5 GHz looks promising it is difficult to find definite observational evidence of effects under study. Namely,

the July 9, 1996 burst can be generated by gyro-synchrotron or/and plasma emission mechanisms and the present model is valid only for the radiation of the plasma emission origin. Therefore, only the plasma emission component, if present, is influenced by this optical thickness reduction. Although due to the presence of particle beams at this phase of the flare an existence of the plasma emission is highly probable, its ratio to the gyro-synchrotron emission is difficult to estimate.

Acknowledgements. This work was supported through the key projects K1-003-601 and K1-043-601, and the grant A3003707 of the Academy of Sciences of the Czech Republic. The author would like to thank the referee for useful comments which helped to improve this paper.

References

Alvarez, H., Haddock, F.T. 1973, Solar Phys., 29, 197
Antonucci, E., Gabriel, A.H., Acton, L.W., Culhane, J.L., Doyle, J.G., Leibacher, J.W., Machado, M.E., Orwig, L.E., Rapley, C.G. 1982, Solar Phys., 78, 107
Antonucci, E., Gabriel, A.H., Dennis, B.R.: 1984, ApJ, 287, 917
Antonucci, E., Dodero, M.A., Martin, Martin, R., Peres, G., Reale, F., Serio, S. 1993, ApJ, 413, 786
Aschwanden, M. J., Benz, A.O. 1995, ApJ, 438, 997
Canfield, R.C. et al. 1980, Solar Flares, Skylab Workshop II, ed. P.A. Sturrock, Boulder, Colorado Assoc. Univ. Press, 231
Doshek, G.A., Cheng, C.C., Oran, E.S., Boris, J.P., Mariska, J.T. 1983, ApJ, 265, 1103
Hori, K., Yokoyama,T., Kosugi,T., Shibata, K. 1997, ApJ, 489, 426
Karlický, M. 1990, Solar Phys., 130, 347
MacNeice, P., McWhirter, R.W.P., Spicer, D.C., Burgess, A. 1984, Solar Phys., 90, 357
Mariska, J.T., Emslie, A.G., Li, P. 1989, ApJ, 341, 1067
Peres, G., Reale, F. 1993, A&A, 267, 566
Somov, B.V. 1992, Physical Processes in Solar Flares, Kluwer Acad. Publ., Dortdrecht, The Netherlands
Zheleznyakov, V.V. 1977, Elektromagnitnyje volny v kosmicheskoj plazme, Nauka, Moscow (in russian)